11-18-2005

Negative Spin Polarization and Large Tunneling Magnetoresistance in Epitaxial Co|SrTiO$_3$|Co Magnetic Tunnel Junctions

Julian P. Velev
University of Nebraska-Lincoln, julian.velev@unl.edu

Kirill D. Belashchenko
University of Nebraska-Lincoln, belashchenko@unl.edu

Derek A. Stewart
Cornell University, stewart@cnf.cornell.edu

Mark van Schilfgaarde
Arizona State University, mark.van_schilfgaarde@kcl.ac.uk

Sitaram Jaswal
University of Nebraska, sjaswal1@unl.edu

See next page for additional authors

Follow this and additional works at: https://digitalcommons.unl.edu/mrsecfacpubs

Part of the Materials Science and Engineering Commons

Authors

Julian P. Velev, Kirill D. Belashchenko, Derek A. Stewart, Mark van Schilfgaarde, Sitaram Jaswal, and Evgeny Y. Tsymbal

P H Y S I C A L   R E V I E W   L E T T E R S

Negative Spin Polarization and Large Tunneling Magnetoresistance in Epitaxial Co|SrTiO₃|Co Magnetic Tunnel Junctions

J. P. Velev,[1] K. D. Belashchenko,[1] D. A. Stewart,[2] M. van Schilfgaarde,[3] S. S. Jaswal,[1] and E. Y. Tsymbal[1]

[1]*Department of Physics and Astronomy and Center for Materials Research and Analysis, University of Nebraska-Lincoln, Lincoln, Nebraska 68588, USA*
[2]*Cornell Nanoscale Science and Technology Facility, Cornell University, Ithaca, New York 14853, USA*
[3]*Department of Chemical and Materials Engineering, Arizona State University, Tempe, Arizona 85287, USA*
(Received 24 August 2005; published 15 November 2005)

We perform an *ab initio* study of spin-polarized tunneling in epitaxial Co|SrTiO₃|Co magnetic tunnel junctions with bcc Co(001) electrodes. We predict a large tunneling magnetoresistance in these junctions, originating from a mismatch in the majority- and minority-spin bands both in bulk bcc Co and at the Co|SrTiO₃ interface. The intricate complex band structure of SrTiO₃ enables efficient tunneling of the minority *d* electrons which causes the spin polarization of the Co|SrTiO₃ interface to be negative in agreement with experimental data. Our results indicate that epitaxial Co|SrTiO₃|Co magnetic tunnel junctions with bcc Co(001) electrodes are a viable alternative for device applications.

Magnetic tunnel junctions (MTJ) are currently the subject of intense study because of their potential application in magnetic random-access memory and magnetic field sensors. An MTJ consists of two ferromagnetic electrodes separated by an insulating barrier. A reversal of the magnetic orientation of the electrodes from antiparallel to parallel by applied magnetic field produces a large change in the electrical resistance of the MTJ. The tunneling magnetoresistance (TMR) is defined by $\text{TMR} = (G_\text{P} - G_\text{AP})/G_\text{AP}$, where G_P and G_AP are the conductances measured for the parallel and the antiparallel magnetization of the electrodes. The origin of this phenomenon is spin-dependent tunneling (SDT), i.e., an imbalance in the electric current carried by electrons with different spin projections (for reviews see Refs. [1,2]).

Larger values of TMR are beneficial for applications. Over the past years the majority of experiments were performed using an amorphous Al₂O₃ barrier because it is relatively easy to deposit as a thin uniform layer. Interest in SDT dramatically increased recently due to the reports of large TMR values about 200% in crystalline Fe|MgO|Fe-based MTJs at room temperature [3].

TMR is often interpreted in terms of the Jullière's formula [4], $\text{TMR} = 2P_1 P_2/(1 - P_1 P_2)$, where P_1 and P_2 are the spin polarizations associated with the two electrodes as measured using the Tedrow-Meservey technique [5]. It was thought that the spin polarization (SP) is determined solely by intrinsic properties of the ferromagnetic electrodes, such as the total density of states (DOS) [4] or the DOS of itinerant bands [6] at the Fermi energy. However, later it became clear that not only the electronic structure of the ferromagnets, but also the bonding at the ferromagnet/insulator interface [7,8] and the evanescent states in the insulator [9,10] control the tunneling SP. It is now commonly accepted that the SP entering the Jullière's formula is due to the ferromagnet/barrier com-plex rather than the ferromagnet alone. This approach has recently been given a theoretical justification [11].

The decisive contribution to this understanding of SDT was due to the work of de Teresa *et al.* [12], who found that the tunneling SP depends on the insulating barrier. They used a half-metallic La₀.₇Sr₀.₃MnO₃ (LSMO) as a spin detector in Co|Al₂O₃|LSMO and Co|SrTiO₃|LSMO MTJs. Since LSMO has only majority states at the Fermi energy, its tunneling SP is positive and close to 100%, regardless of the insulating barrier. As expected, Co|Al₂O₃|LSMO MTJs were found to have a normal TMR. Surprisingly, Co|SrTiO₃|LSMO MTJs showed *inverse* TMR. De Teresa *et al.* proposed that the SP of the Co|SrTiO₃ interface must be negative, opposite to that of the Co|Al₂O₃ interface. They interpreted the sign change of the SP in terms of interface bonding [7], arguing that it allows efficient tunneling of *d* electrons across the SrTiO₃ barrier. However, until now no quantitative understanding of this phenomenon has been offered. A large negative SP obtained for the Co|SrTiO₃ interface in these experiments indicates that SrTiO₃ holds much promise for the use in transition-metal based MTJs such as Co|SrTiO₃|Co.

In this Letter, we analyze spin-dependent tunneling in epitaxial Co|SrTiO₃|Co(001) MTJs using first-principles band structure methods. We demonstrate that these junctions have a very large TMR due to a mismatch in the electronic bands of the majority- and minority-spin electrons both in bulk bcc Co and at the Co|SrTiO₃ interface. We show that the complex band structure of SrTiO₃ enables efficient tunneling of the minority *d* electrons from Co, causing the SP of the conductance to be negative which explains the experiments of de Teresa *et al.* This is very different from MTJs based on *sp*-bonded insulators, such as Al₂O₃ and MgO, in which the tunneling current is dominated by majority-spin carriers.

Our method employs the structural model of Co|SrTiO$_3$|Co MTJ obtained by Oleinik *et al.* [13] and shown in Fig. 1. This minimum-energy structure was found by relaxing atomic structures of the MTJ with different interfaces between fcc Co(001) and SrTiO$_3$(001). The experimental lattice parameters of bulk fcc Co and bulk SrTiO$_3$ in its equilibrium perovskite structure are 3.55 and 3.91 Å, respectively. The 10% lattice mismatch would normally prevent epitaxial growth. However, good metals usually accommodate various lattice structures with only a small energetic penalty because their binding energy depends primarily on density. Cobalt assumes hcp structure in bulk and fcc structure in thin films. It can also be grown in bcc structure on a Cr substrate [14] and on GaAs or Ge substrates covered with an Fe seed layer [15]. The equilibrium lattice parameter of bcc Co is 2.83 Å [16] which has only a 2.3% mismatch with the SrTiO$_3$ lattice rotated through 45° around the [001] axis. Therefore, in the calculation of Oleinik *et al.* [13], the strained Co layer proceeded along the Bain path from the fcc to the slightly distorted bcc structure. It is therefore likely that the top Co electrode in the experiments of de Teresa *et al.* [12] grew in the bcc phase on SrTiO$_3$, and that fully crystalline bcc Co|SrTiO$_3$|Co MTJs may be grown on a suitable substrate.

We calculate the electronic structure using the tight-binding linear muffin-tin orbital method in the atomic sphere approximation [17] and the local density approximation for the exchange-correlation energy. The conductance is obtained using the principal-layer Green's function technique [18]. The spin-resolved conductance of a Co|SrTiO$_3$|Co MTJ is shown in Fig. 2 as a function of barrier thickness. It is seen that the conductance decreases exponentially with a similar decay length for a parallel and antiparallel configuration of the electrodes. The conductance of the minority-spin channel in the parallel configuration $G_{\downarrow\downarrow}$ is greater than that of the majority-spin channel $G_{\uparrow\uparrow}$, or of any spin channel in the antiparallel configuration $G_{\uparrow\downarrow}$. The SP of the conductance in the parallel configuration, $P = (G_{\uparrow\uparrow} - G_{\downarrow\downarrow})/(G_{\uparrow\uparrow} + G_{\downarrow\downarrow})$, is negative for all barrier thicknesses [see P(MTJ) in Fig. 2]. Moreover, except

for the thinnest barrier of 3 monolayers (ML), P is almost constant at -90%, and the TMR is very high (about 2000% for 7 and 11 MLs, and about 1000% for 15 MLs).

The fact that the tunneling current is dominated by minority-spin electrons can be explained by taking into account the band structure of bcc Co and decay rates of the Co states in SrTiO$_3$. The majority-spin $3d$ band in bcc Co is filled, so that the DOS at the Fermi level has a large negative SP [19]. If the $3d$ states could efficiently tunnel through the barrier, the tunneling SP would also be negative. As seen from the complex band structure of SrTiO$_3$, shown in Fig. 3 at the $\bar{\Gamma}$ point ($\mathbf{k}_{\parallel} = 0$), the Δ_5 and Δ_1 states have comparable decay rates in the gap of SrTiO$_3$. Therefore, both the majority-spin Δ_1 band and the minority-spin Δ_5 band of bcc Co [19] can tunnel efficiently through the SrTiO$_3$ barrier. This is different from Fe|MgO|Fe tunnel junctions [10] in which tunneling from the $3d$ states is filtered out by selection rules related to the complex band structure of MgO [9].

While the $\bar{\Gamma}$ point analysis is instructive, it is not sufficient because the conductance is not dominated by this point. This fact can be understood from Fig. 4, showing the three lowest decay rates of the evanescent states at the Fermi energy. It is seen that a very large area of the Brillouin zone, forming a cross pattern along the $\bar{\Gamma}\bar{M}$ directions, exhibits two lowest decay rates that are very close to those at the $\bar{\Gamma}$ point. Clearly, at large barrier thickness the states lying in this "cross" area should dominate the conductance. This feature is in sharp contrast to sp-bonded insulators like MgO and Al$_2$O$_3$ where the decay rate has a deep parabolic minimum in the vicinity of the $\bar{\Gamma}$ point. This difference is due to the conduction band of SrTiO$_3$ being formed by fairly localized $3d$ states of Ti instead of free-electron-like states of a metal atom in simple oxides. Obviously, these properties of the SrTiO$_3$ complex band structure exclude efficient symmetry-related spin filtering. Therefore, the minority-spin d states which
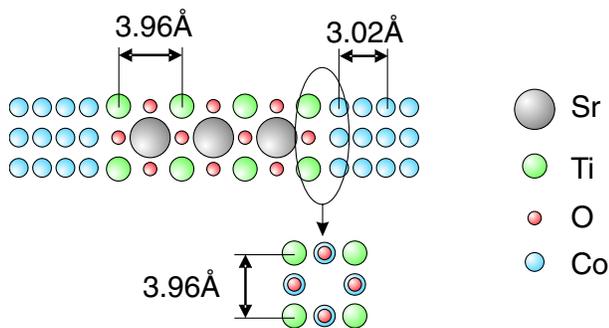

FIG. 1 (color online). Schematic graph of the most stable interface structure of the Co|SrTiO$_3$|Co(001) MTJ taken from Ref. [13]. Projections on two perpendicular planes are shown.
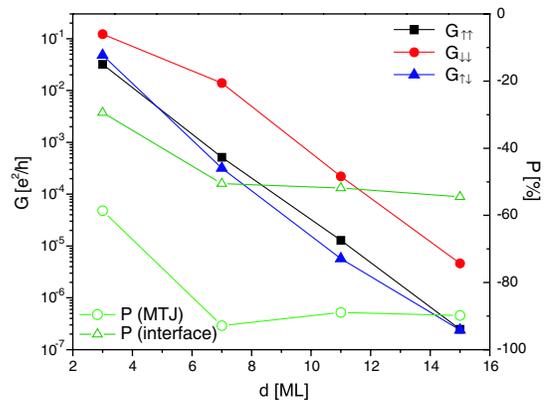

FIG. 2 (color online). Conductance G (solid symbols) and spin polarization P (open symbols) vs barrier thickness d for a Co|SrTiO$_3$|Co MTJ.
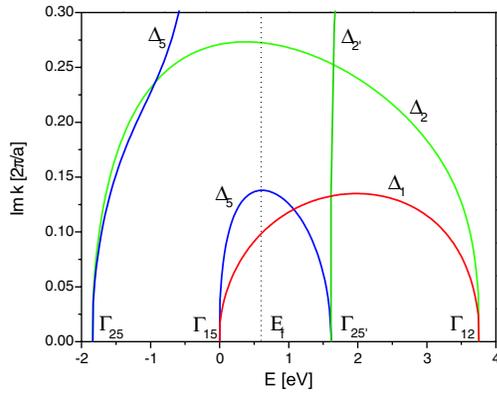
FIG. 3 (color online).   Complex band structure of $SrTiO_3$ at the $\bar{\Gamma}$ point. The position of the Fermi level E_f in a Co|$SrTiO_3$|Co MTJ is shown by a dashed line.

have much larger DOS at the Fermi energy than the majority-spin states dominate the conductance providing a negative SP of the tunneling current in Co|$SrTiO_3$|Co MTJs.

Figure 5 shows the conductance of a Co|$SrTiO_3$|Co MTJ as a function of $\mathbf{k}_{\parallel}$ for two barrier thicknesses. The details in this figure can be understood by comparing it with the $\mathbf{k}_{\parallel}$-resolved DOS in the Co electrodes shown in Fig. 6. The majority-spin DOS can be viewed as projection of the Fermi-surface octahedron with rounded edges folded into a smaller Brillouin zone. The central star-shaped area in Fig. 6(a) has two bulk eigenstates per $\mathbf{k}_{\parallel}$. Areas adjacent on the four sides have two additional eigenstates per $\mathbf{k}_{\parallel}$. Close to the boundary between these two areas there is a van Hove singularity enhancing the DOS. This enhancement is clearly reflected in Fig. 5(a). Similar anomalies are visible close to the Brillouin zone corners and diagonals. For the thicker barrier of 11 MLs the cross pattern from the $SrTiO_3$ complex band structure reveals itself in Fig. 5(d).

As is seen from Figs. 5(b) and 5(e), the main contribution to the minority-spin conductance comes from the extended area around the $\bar{\Gamma}$ point. Comparing Figs. 5(b) and 6(b), we can see that for 3 MLs of $SrTiO_3$ this contribution is generated by specific Fermi-surface sheets. These sheets have the shape of two identical ellipsoids that are superimposed by a 90° rotation around the tetragonal
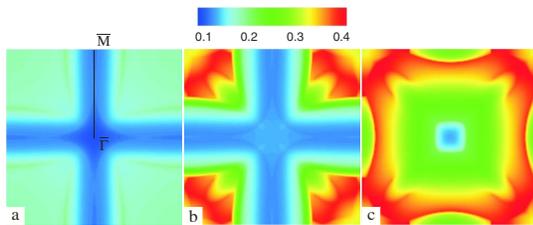

FIG. 5 (color online).   Conductance (in units of e^2/h) as a function of $\mathbf{k}_{\parallel}$ for Co|$SrTiO_3$|Co MTJs with 3 (a)–(c) and 11 MLs (d)–(f) of $SrTiO_3$. (a),(d) Majority- and (b),(e) -minority-spin channels in the parallel configuration; (c),(f) either spin channel in the antiparallel configuration.

axis (not shown). They project as two crossed ellipses in Fig. 6(b) and dominate the transmission in Fig. 5(b). Additional square-shaped features in immediate vicinity [Fig. 5(b)] come from interface resonant states split off from these bulk sheets. These interface states are seen in Fig. 7(a). They move somewhat closer to the $\bar{\Gamma}$ point as the barrier thickness increases [Figs. 7(a) and 7(b)]. For the 11 ML barrier the conductance is dominated by these interface states [cf. Figures 5(e) and 7(c)].

The conductance for the antiparallel configuration [Figs. 5(c) and 5(f)] is generally large at those $\mathbf{k}_{\parallel}$ where the majority- and minority-spin conductances in the parallel configuration are *both* large. This is because tunneling electron must traverse both interfaces. Exceptions may be found close to high-symmetry lines or points like $\bar{\Gamma}$, where symmetries of the states dominating in the two spin channels are incompatible. The comparison of the conductance distribution in the parallel configuration for majority-spin [Figs. 5(a) and 5(d)] and minority-spin [Figs. 5(b) and 5(e)] electrons over the interface Brillouin zone reveals a significant mismatch between the two spin channels. This makes the conductance in the antiparallel configuration

FIG. 4 (color online).   Three lowest decay rates (in units of $2\pi/a$) of the evanescent states in $SrTiO_3$ as a function of $\mathbf{k}_{\parallel}$ at the Fermi energy.
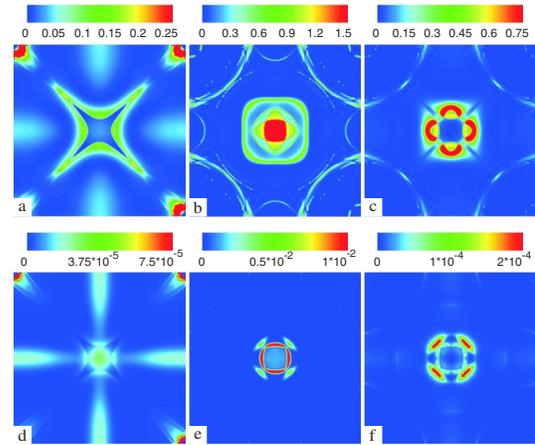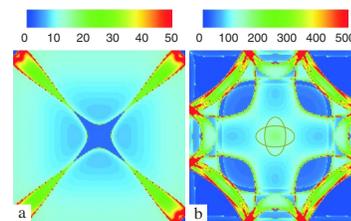

FIG. 6 (color online). $\mathbf{k}_{\parallel}$-resolved DOS (arbitrary units) of bcc Co considered as simple tetragonal lattice with 2 atoms per cell. (a) Majority-spin electrons; (b) minority-spin electrons.
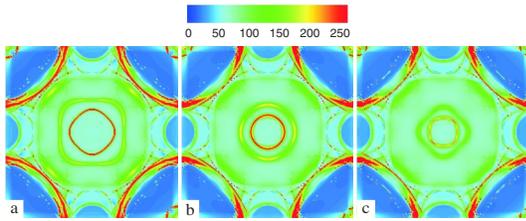
FIG. 7 (color online). Minority-spin DOS (arbitrary units) for the interfacial Co layer in Co|SrTiO$_3$|Co MTJs with barrier thickness of (a) 3, (b) 7, and (c) 11 MLs. Interface resonant states reveal themselves as two rings closest to the $\bar{\Gamma}$ point.

much smaller than the conductance in the parallel configuration resulting in a very large TMR.

Now we make a quantitative comparison of our results with the experiments of de Teresa *et al.* [12] who found that the SP of the Co|SrTiO$_3$ interface is -25%. We determine the SP of the interface from the metal-induced DOS in the barrier. In doing this, we approximate the LMSO electrode as an ideal spin analyzer, similar to the Tersoff-Hamann model for an STM tip [20], and assume that the DOS in the barrier is simply the sum of DOS induced by the left and right electrodes (this is valid as long as the barrier is not too thin). Since in our case pure surface states are absent, all the barrier DOS is metal-induced. Therefore, we can use the total DOS in the middle of the barrier with no ambiguity. The SP of the Co|SrTiO$_3$ interface obtained in such a way is close to -50% and is almost independent of barrier thickness [see P (interface) in Fig. 2]. A separate calculation for 11 ML barrier shows that the SP is a smooth function of energy and it is negative within a large interval around the Fermi energy. Thus, our model explains the negative value of the SP of the Co|SrTiO$_3$ interface obtained by de Teresa *et al.*; some quantitative differences may be related to the effects of disorder unavoidable in experiment.

Finally we note that the predicted properties of Co|SrTiO$_3$|Co MTJs are very sensitive to the atomic structure of Co and SrTiO$_3$. This fact is supported by recent experiments studying spin-dependent tunneling from fcc Co across an *amorphous* SrTiO$_3$ barrier [21]. It was found that the SP of the Co|SrTiO$_3$ interface is positive similar to that of Co|Al$_2$O$_3$. This result might be the consequence of O atoms adsorbed by the Co surface as was recently predicted for Co|Al$_2$O$_3$|Co MTJs [22].

In conclusion, we have predicted a very large TMR in epitaxial Co|SrTiO$_3$|Co MTJs with bcc Co(001) electrodes, originating from a mismatch of majority- and minority-spin states contributing to the conductance. We found a large negative tunneling spin polarization of the Co|SrTiO$_3$(001) interface in agreement with experimental data. We attributed this property to the complex band structure of SrTiO$_3$ which is formed from localized 3d states of Ti and hence allows efficient tunneling of the

minority d electrons of Co. This behavior is a drastic departure from the mechanism of tunneling in MTJs based on sp-bonded insulators supporting conduction of majority-spin electrons. It is highly desirable to study experimentally other insulators, whose band gap is controlled by the bonding of valence d electrons, and hence their complex band structure may promote negative tunneling SP in MTJs. The large TMR and relatively high conductance suggest that MTJs based on SrTiO$_3$ may provide a viable alternative to MgO- and Al$_2$O$_3$-based MTJs for device applications.

[1] E. Y. Tsymbal, O. N. Mryasov, and P. R. LeClair, J. Phys. Condens. Matter **15**, R109 (2003).
[2] X.-G. Zhang and W. H. Butler, J. Phys. Condens. Matter **15**, R1603 (2003).
[3] S. S. P. Parkin *et al.*, Nat. Mater. **3**, 862 (2004); S. Yuasa *et al.*, Nat. Mater. **3**, 868 (2004); D. Djayaprawira *et al.*, Appl. Phys. Lett. **86**, 092502 (2005).
[4] M. Jullière, Phys. Lett. A **54**, 225 (1975).
[5] P. Tedrow and R. Meservey, Phys. Rev. B **7**, 318 (1973).
[6] M. B. Stearns, J. Magn. Magn. Mater. **5**, 167 (1977).
[7] E. Y. Tsymbal and D. G. Pettifor, J. Phys. Condens. Matter **9**, L411 (1997).
[8] E. Y. Tsymbal and K. D. Belashchenko, J. Appl. Phys. **97**, 10C910 (2005).
[9] Ph. Mavropoulos, N. Papanikolaou, and P. H. Dederichs, Phys. Rev. Lett. **85**, 1088 (2000).
[10] W. H. Butler *et al.*, Phys. Rev. B **63**, 054416 (2001).
[11] K. D. Belashchenko *et al.*, Phys. Rev. B **69**, 174408 (2004).
[12] J. M. de Teresa *et al.*, Phys. Rev. Lett. **82**, 4288 (1999); Science **286**, 507 (1999).
[13] I. I. Oleinik, E. Y. Tsymbal, and D. G. Pettifor, Phys. Rev. B **65**, 020401(R) (2002).
[14] R. Walmsley *et al.*, IEEE Trans. Magn. **19**, 1992 (1983).
[15] H. Wieldraaijer *et al.*, Phys. Rev. B **67**, 224430 (2003), and references therein.
[16] G. A. Prinz, Phys. Rev. Lett. **54**, 1051 (1985).
[17] O. K. Andersen, Phys. Rev. B **12**, 3060 (1975).
[18] I. Turek *et al.*, *Electronic Structure of Disordered Alloys, Surfaces, and Interfaces* (Kluwer, Boston, 1997); J. Kudrnovský *et al.*, Phys. Rev. B **62**, 15 084 (2000); S. V. Faleev *et al.*, Phys. Rev. B **71**, 195422 (2005).
[19] D. Bagayoko, A. Ziegler, and J. Callaway, Phys. Rev. B **27**, 7046 (1983).
[20] J. Tersoff and D. R. Hamann, Phys. Rev. B **31**, 805 (1985).
[21] A. Thomas, J. S. Moodera, and B. Satpati, J. Appl. Phys. **97**, 10C908 (2005).
[22] K. D. Belashchenko *et al.*, Phys. Rev. B **71**, 224422 (2005).